A Procedure for Determination of Reduced Polytopic Models Based on Robust Multi-Model Representation of Large Dimensions

Carlos A. Cappelletti
Facultad Regional Paraná,
Universidad Tecnológica Nacional,
Paraná, Argentina,
ccappelletti@frp.utn.edu.ar

Hugo A. Pipino, Emanuel Bernardi
Facultad Regional San Francisco,
Universidad Tecnológica Nacional,
San Francisco, Argentina,
hpipino@sanfrancisco.utn.edu.ar
ebernardi@sanfrancisco.utn.edu.ar

Eduardo J. Adam
Facultad de Ingeniería Química,
Universidad Nacional del Litoral,
Santa Fe, Argentina,
eadam@fiq.unl.edu.ar

***Abstract*—This study entails a meticulous examination of the dynamic characteristics exhibited by the continuous stirred tank reactor (CSTR) with the objective of establishing a robust multi-model representation that accurately captures the reactor behavior across its operational range. To achieve this, a methodology is presented, which incorporates parameter variations as uncertainties within the model. The result is a concise polytopic representation, reduced to its vertices, that effectively captures the system dynamics and encompasses the range of parameter uncertainties.**

***Index Terms*—robust multi-model representation, linear parameter-varying, nonlinear system, CSTR**

I. Introduction

In the field of classical process control ([1]–[3], among others), it is widely acknowledged that the nonlinear nature and sluggish dynamic responses exhibited by industrial processes needs the tuning of controllers/regulators that offer robustness to the control system. This robustness is essential for addressing the inherent uncertainties associated with process modeling. The complexity increases when process constraints are taken into account. In response to this challenge, traditional process control approaches rely on the tuning of industrial controllers using conventional techniques, which often result in conservative dynamic responses [4].

Within the literature, various control strategies can be found that utilize a multi-model approach for representing nonlinear plants [5]–[7]. This approach involves representing nonlinear systems using a finite set of linear models, where the effects of nonlinearity are captured through the inclusion of linear time-invariant (LTI) models corresponding to different operating points.

The conventional approach to obtaining a polytopic representation involves the construction of a polytope, as a convex hull, that encapsulates the entire operating range of the nonlinear model, and subsequently augmenting the model with an additional matrix that take into account the external disturbances ([8] and [9]). In contrast to this method, this article proposes a novel procedure to incorporate all parameter variations. That is, covering the both aspects, the changes in the operating points and the presence of external disturbances, as sources of model uncertainty. Consequently, they are included in a reduced polytopic representation.

As a consequence, this paper focuses on the development of a polytopic representation for a Continuous Stirred Tank Reactor (CSTR). Furthermore, an extension of the multi-objective regulator proposed in [10] is introduced, which incorporates a discrete-time representation. Consequently, the linear matrix inequality (LMI) formulations involved in the regulator design differs from those in the continuous-time case.

This work is organized as detailed below. In Section II the nonlinear model of the CSTR is presented, showing, through numerical simulations, its nonlinear dynamics. Then, in Section III a procedure to build a reduced polytopic model is presented. Subsequently, in Section IV three LQR regulators are analyzed, where two of them are designed with variable gain using LMI. Moreover, in Section V the dynamic behavior of the feedback system is studied, through numerical simulations. Finally, the conclusions are presented in Section VI.

II. Nonlinear Behavior of CSTR Dynamic

In this section, the CSTR presented by Morningred et al. [11] is considered and depicted in Fig. 1.

The nonlinear model for this unit operation results:

$$\dot{C_A}(t) = \frac{q_e(t)}{V^0}\left(C_{Ae} - C_A(t)\right) - k_0 e^{\frac{-E_R}{T(t)}} C_A(t)\,, \tag{1}$$

$$\begin{aligned}\dot{T}(t) =& \frac{q_e(t)}{V^0}\left(T_e - T(t)\right) + k_1 e^{\frac{-E_R}{T(t)}} C_A(t) \\ &+ \frac{q_c(t)}{V^0} k_2 \left(1 - e^{\frac{-k_3}{q_c(t)}}\right)\left(T_{ce} - T(t)\right)\,,\end{aligned} \tag{2}$$

where $k_1 = -\frac{\Delta H k_0}{\rho C_p}$, $k_2 = \frac{\rho C_{pc}}{\rho_c C_p}$ and $k_3 = \frac{h_A}{\rho_c C_{pc}}$. Based on its operative conditions, in Table I is shown the physical and operational parameters.

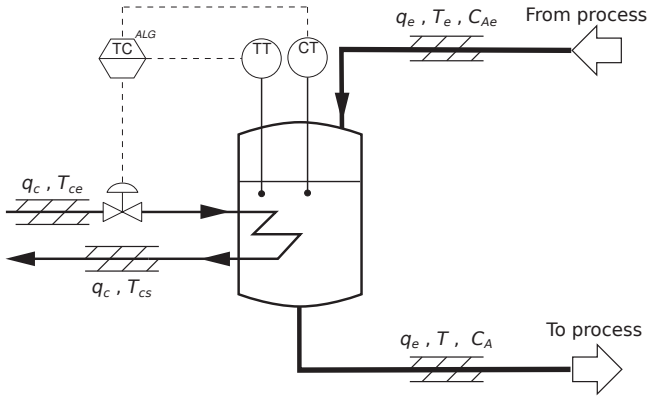

Fig. 1: Diagram of a CSTR and its corresponding temperature controller.

TABLE I: Parameters of the CSTR process.

Name	Description	Value
V^0	Volume	100 L
q_e	Feed flow rate	100 L min^{-1}
T_e	Feed temperature	350 K
C_{Ae}	Feed concentration	1 mol L^{-1}
T_{ce}	Inlet coolant temp.	350 K
E/R	Activation energy	1e4 K
ΔH	Heat of reaction	-2e5 cal mol^{-1}
C_p, C_{pc}	Specific heats	1 cal g^{-1} K^{-1}
ρ, ρ_c	Liquid densities	1e3 g L^{-1}
h_A	Heat transfer term	7e5 cal min^{-1} K^{-1}
k_0	Reaction rate constant	7.2e10 L min^{-1}

A. *Reactor behavior in open-loop*

In order to gain insights into the dynamics of this nonlinear open-loop system, various initial and steady state conditions are considered, with the specie A concentration ($C_{A_{ss}}$), ranging from 0.05 to 0.14 mol/L. This range is chosen to comprehensively analyze the entire operating range of the system. Consequently, the states that represent the reactor dynamics are disturbed in two opposing directions. Specifically, two distinct operating points are examined in detail, and their characteristics are elaborated upon below.

- **Test-Part 1.** Initially, it is considered that the CSTR has an outlet reactant concentration $C_{A_{ss}} = 0.14$ mol L^{-1} and a new steady state for the outlet concentration $C_{A_{ss}} = 0.05$ mol L^{-1} is pretended to reach. To do this, it is proposed to use the coolant flow rate that corresponds to the new desired reactant concentration.
- **Test-Part 2.** In this case, an opposite situation to the previous one is considered. That is, to bring up the concentration $C_{A_{ss}} = 0.05$ mol L^{-1} to $C_{A_{ss}} = 0.14$ mol L^{-1}, changing the refrigerant flow with the same criteria of the previous test. Thus, the coolant flow necessary to reach the desired concentration ($C_{A_{ss}} = 0.14$ mol L^{-1}) is supplied to the reactor.

Thus, it becomes apparent how variations in the reactant concentration influence the dynamic behavior of the CSTR within the specified operating range of this particular variable ($\Delta C_A(0) = \pm 0.09$ mol L^{-1}).

The results of these simulations are shown in Figs. 2 to 5. Clearly, the nonlinear behavior of the reactor is evident when trying to reach the two equilibrium points mentioned above.

In Figs. 2 and 3 (blue lines) it is observed that when the outlet concentration $C_{A_{ss}} = 0.14$ mol L^{-1} is changed to $C_{A_{ss}} = 0.05$ mol L^{-1}, the system quickly reaches the desired steady state increasing the temperature inside the reactor until reach the equilibrium point (Fig. 4 - blue line). However, according to the simulation results (Figs. 2 and 3 - red lines) when trying to change $C_{A_{ss}} = 0.05$ mol L^{-1} to $C_{A_{ss}} = 0.14$ mol L^{-1} the system does not reach the steady state during the chosen simulation time, because this point is close to a marginal stable equilibrium point for the open-loop CSTR due to the reaction curve and the red heat dissipation line become tangent (Fig. 5).

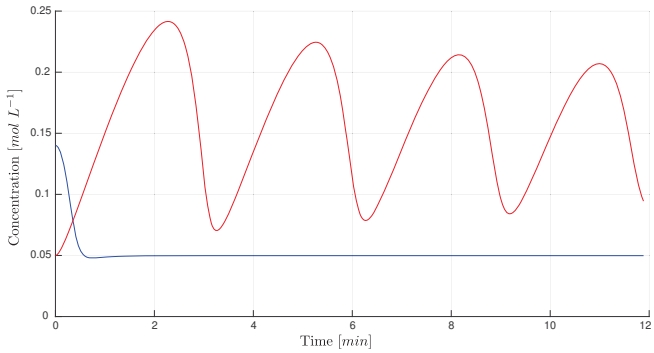

Fig. 2: Concentration dynamic responses of CSTR.

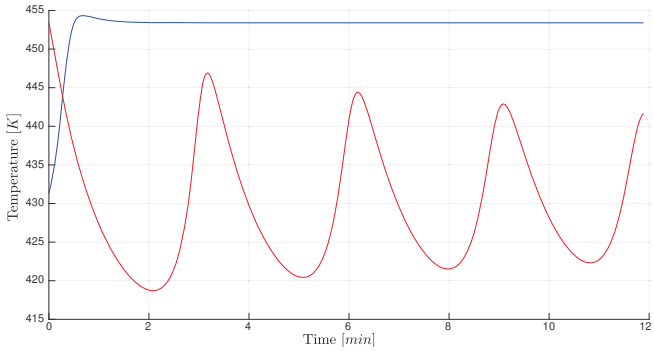

Fig. 3: Temperature dynamic responses of CSTR.

III. CSTR POLYTOPIC MODELS WITH PARAMETRIC UNCERTAINTY

In this section, it is analyzed the challenges of approximating a nonlinear physical system with a nominal linear model and compensating for the associated parametric uncertainty. One approach for designing a regulator for such a system involves constructing a polytope, as a convex hull, that encloses the nominal nonlinear plant over its entire operating range and incorporating a matrix to model parameter variations as a disturbance vector. Although considering the maximum variation in the input parameters, the original polytope has 94

ISBN: 978-950-766-230-0

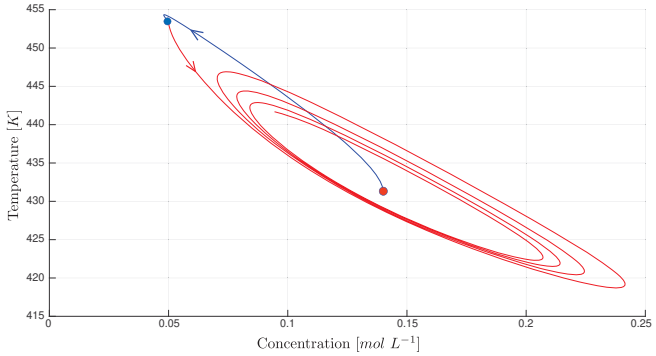

Fig. 4: State space corresponding to the two studied test.

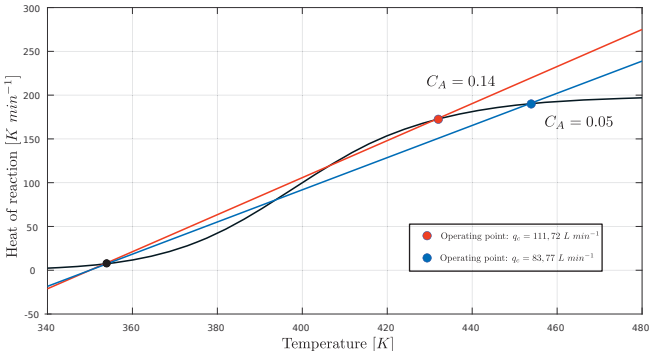

Fig. 5: Reaction and dissipation heat curves.

vertices (Fig. 6), where each one is associated to an identified LTI model. However, by mean of proposed procedure eight plants where determined in the operating region as shown below. In this way, it is possible to reduce the computational limitations reducing the number of vertices while maintaining the robustness of the control system.

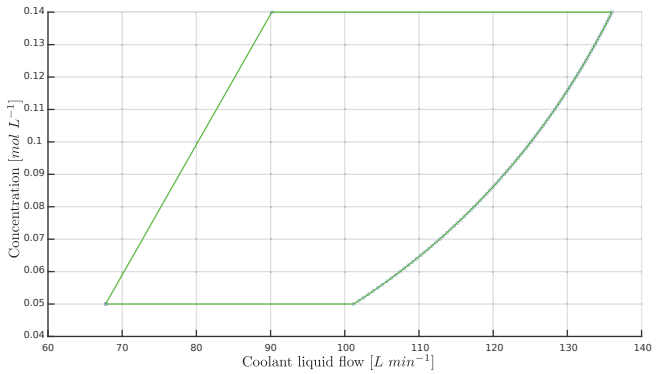

Fig. 6: Original operating region (94 vertices)

A. *Procedure to build a reduced polytopic model.*

In order to reduce the number of vertex operating points on a convex region obtained from the dynamic responses of a disturbed nonlinear system, this article proposes the implementation of a general procedure. The applied procedure is represented schematically in Fig. 7 and it is detailed below.

Proposed procedure

1) Consider three vertices, for example v_1, v_2 and v_3.
2) Compute the angles θ_1 and θ_2, if the angular difference is less than a predetermined value, v_2 is deleted and go to step 3. Otherwise, v_2 is not omitted and go to Step 4. Take into account that,
   a) when several consecutive vertices are suppressed, the angular difference is increased with respect to the original θ_1, but as long as the bound for the angular difference is not exceeded, the consecutive vertices will be deleted. When this angular limit is exceeded, the last vertex is not discarded, considering this and the two next vertex, go to Step 2.
   b) The bound imposed on this angular difference depend on some criterion imposed for the designer.
3) If v_2 is deleted, rename v_3 as v_2 and go to next step.
4) Taking into account the last not discarded two vertices as the initial vertices, the procedure is continued with the next vertex.

The final result of applying this procedure to the polytopic operating region associated with the reactor is shown in Fig. 8. Now, the reduced region, which is an approximation of the original operating region, has only eight vertex operation points with significant difference between them.

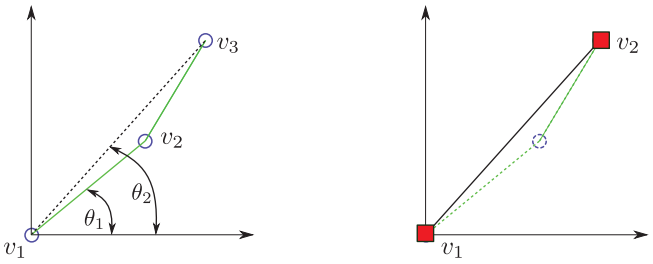

Fig. 7: Vertex reduction

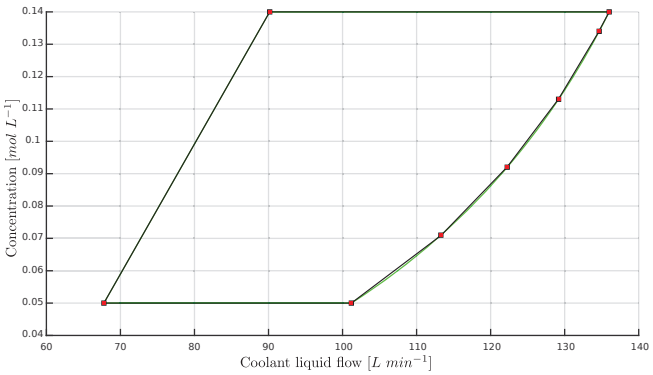

Fig. 8: Reduced operating region (8 vertices)

B. *Discrete-time polytopic model*

According to the results from the previous section and considering a bounded parameters variation, the eight LTI

models corresponding to the obtained operating points were determined.

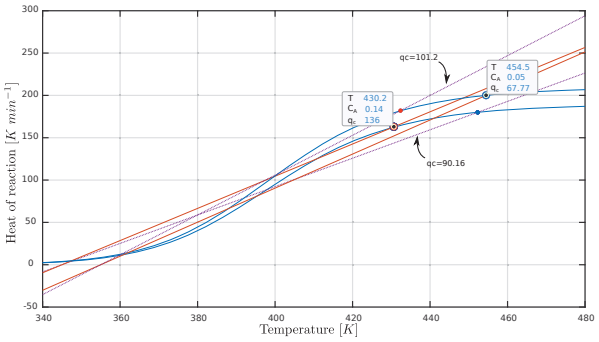

Fig. 9: Sigmoid and dissipation heat functions.

Thereby, for a variation of $\pm 5\%$ in the three system parameters (C_{A_e}, T_e and T_{c_e}), the value range for the concentration C_A under analysis corresponds to the temperature range $430.2\ \mathrm{K} \leq T \leq 454.5\ \mathrm{K}$.

By mean of Fig. 9 it was determined that the temperature range is achieved when the coolant flow is $67.77\ \mathrm{L\,min^{-1}} \leq q_c \leq 136\ \mathrm{L\,min^{-1}}$, where the equilibrium points bound the operating interval over the reaction curve.

Then, linearizing the differential equations (1) and (2) in the working range, the eight LTI vertex models are obtained. Table II shows the matrices A_j and B_j, from the LTI vertex models. These models constitute the vertices of the polytopic model with uncertainties for the CSTR.

LTI Model	A_j	B_j
1	$\begin{pmatrix} 0.5129 & -0.0011 \\ 90.5390 & 1.1699 \end{pmatrix}$	$\begin{pmatrix} 0 \\ -0.0351 \end{pmatrix}$
2	$\begin{pmatrix} 0.5131 & -0.0011 \\ 90.0292 & 1.1580 \end{pmatrix}$	$\begin{pmatrix} 0 \\ -0.0347 \end{pmatrix}$
3	$\begin{pmatrix} 0.5927 & -0.0013 \\ 74.2560 & 1.1975 \end{pmatrix}$	$\begin{pmatrix} 0 \\ -0.0300 \end{pmatrix}$
4	$\begin{pmatrix} 0.6704 & -0.0014 \\ 58.9150 & 1.2088 \end{pmatrix}$	$\begin{pmatrix} 0 \\ -0.0281 \end{pmatrix}$
5	$\begin{pmatrix} 0.7239 & -0.0014 \\ 48.3758 & 1.2145 \end{pmatrix}$	$\begin{pmatrix} 0 \\ -0.0265 \end{pmatrix}$
6	$\begin{pmatrix} 0.7629 & -0.0015 \\ 40.7064 & 1.2170 \end{pmatrix}$	$\begin{pmatrix} 0 \\ -0.0252 \end{pmatrix}$
7	$\begin{pmatrix} 0.7720 & -0.0015 \\ 39.1695 & 1.2340 \end{pmatrix}$	$\begin{pmatrix} 0 \\ -0.0258 \end{pmatrix}$
8	$\begin{pmatrix} 0.7721 & -0.0015 \\ 38.8856 & 1.2173 \end{pmatrix}$	$\begin{pmatrix} 0 \\ -0.0248 \end{pmatrix}$

TABLE II: LTI vertex models of the polytope.
Note: $C = (1 \quad 0)$ and $D = 0$ for all models.

Thus, the robust discrete-time model is determined as follows:

$$\begin{aligned} x(k+1) &= A(\eta(k))x(k) + B(\eta(k))u(k), \\ y(k) &= Cx(k) + Du(k), \\ x(0) &= x_0, \end{aligned} \tag{3}$$

where the matrices $A(\eta(\cdot))$ and $B(\eta(\cdot))$ depend on the parameter $\eta(\cdot)$, and the matrices C and D are considered known and constant. Also, $x \in \mathbb{R}^2$ is the state vector ($[C_A \quad T]'$), $u \in \mathbb{R}^1$ is the manipulated variable (q_c), $A \in \mathbb{R}^{2\times 2}$ is the state matrix, $B \in \mathbb{R}^{2\times 1}$ is the input matrix, $C \in \mathbb{R}^{1\times 2}$ the output matrix, $D = 0$ and η is a nonlinear parameter vector that takes in account the nonlinearities of Eqns. (1) and (2) and the time variation of their input parameters ([12]).

Based on the interpolation of the vertex LTI models, it is possible to obtain a model inside the polytopic operating region:

$$\begin{aligned} A(\eta(k)) &= \sum_{j=1}^{n_m} \alpha_j(k) A_j, \\ B(\eta(k)) &= \sum_{j=1}^{n_m} \alpha_j(k) B_j, \\ \sum_{j=1}^{n_m} \alpha_j(k) &= 1, \quad \forall t \geq 0. \end{aligned} \tag{4}$$

where $n_m = 8$, α_j is a membership vector that relates the uncertain Linear Parameter-Varying (LPV) model to the vertex LTI models.

IV. Regulator design with variable gain in discrete-time

This section presents a robust regulator designed with variable gain using LMI. The design contemplates uncertainties in the model parameters and operational constraints.

Firstly, a formulation of an LQR for a discrete-time LTI model is carried out, which uses a static feedback gain vector. Then, the proposed strategy is extended to discrete-time LPV models. Afterwards, amplitude constraints into the manipulated variable are incorporate. Thereafter, the formulation of a robust LQR with constraints is presented and finally the results obtained are extended to a state feedback with variable gain vector.

A. LQR problem formulation using LTI models

Considering the general state-space form discrete-time LTI model:

$$\begin{aligned} x(k+1) &= Ax(k) + Bu(k)\,, \\ y(k) &= Cx(k) + Du(k)\,, \\ x(0) &= x_0\,, \end{aligned} \tag{5}$$

where $x \in \mathbb{R}^n$ are measurable states and $u \in \mathbb{R}^m$ is the control signal with $k = 0, 1, 2, ..., \infty$, and establishing a state feedback control law, given by:

$$u(k) = Fx(k)\,. \tag{6}$$

So, the closed-loop control system becomes:

$$\begin{aligned} x(k+1) &= A_{cl}x(k) \\ x(0) &= x_0\,, \end{aligned} \tag{7}$$

where $A_{cl} \triangleq A + BF$.

ISBN: 978-950-766-230-0

B. LQR problem formulation using LPV models in discrete-time

In this section, the results from Section IV-A, which is based on LTI models, are extended to solve control problems on linear models with parametric uncertainties (LPV).

In this way, a robust control formulation is presented that encloses the parameters variations of the nominal model in an uncertainty model, in consequence the real plant is included within a multi-model framework.

Considering the discrete-time LPV model given by Eqn. (3), it is possible to incorporate the dynamics of the uncertain system into a convex polytope of n_m vertices with an affine dependence on the parameter $\eta(\cdot)$ ([13]):

$$\left[A\left(\eta(k)\right) \mid B\left(\eta(k)\right)\right] \in \Omega, \quad \forall k \geq 0, \tag{8}$$

with Ω is a polytope with LTI models at its n_m vertices, which is represented as:

$$\Omega \triangleq \text{Co}\{\ [A_1 \mid B_1], [A_2 \mid B_2], \ldots, [A_{n_m} \mid B_{n_m}]\ \}. \tag{9}$$

where $\text{Co}\{\cdot\}$ denotes a convex hull and $[A_j \mid B_j]$ are the matrices of each vertex LTI model.

That is, $\forall k \geq 0$ there exist n_m non-negative coefficients $\alpha_j(k)$, with $j = 1, 2, ..., n_m$ such that:

$$\begin{aligned} [A(\eta(k)) \mid B(\eta(k))] &= \sum_{j=1}^{n_m} \alpha_j(k)\ [A_j \mid B_j]\,, \\ \sum_{j=1}^{n_m} \alpha_j(k) &= 1\,. \end{aligned} \tag{10}$$

Subsequently, two LQR controllers are formulated, but due to the document format constraints a detailed description of these controllers cannot be provided in this article.

1) LQR formulation using LTI model (See [14] and [15]).
2) LQR problem using LPV models as an extended version of the regulator described above.

V. Numerical Simulation

For numerical simulation, the nonlinear model given by Eqns. (1) and (2) are employed for simulating the process.

Moreover, the LQR weighting matrices were defined as $R_x = \mathbb{I}$ and $R_u = \mathbb{I}$ [1]. However, it is important to highlight that the three implemented LQR formulations use the same set of matrices, and operate with the same sampling period. In addition, the results of numerical simulation here presented were achieved using MATLAB with Yalmip toolbox ([16]).

For a first test, the reference tracking goal is set as $0.14\ \text{mol}\,\text{L}^{-1}$ for the concentration of A. Additionally, the nominal plant is simulated with an initial disturbance of states given by $\Delta C_A = -0.09\ \text{mol}\,\text{L}^{-1}$ and $\Delta T = 22.08\ \text{K}$.

The states evolution and the coolant flow can be seen in Figs. 10 to 13. There it is shown, in black line, the system response to a disturbance in the states when a static and unconstrained LQR is applied. In Figs. 10, 11 and 12, it can be seen that the system has a good performance with this regulator but, at the same time, in Fig. 13, a coolant flow rate greater than $175\ \text{L}\,\text{min}^{-1}$ is required, exceeding the maximum available.

[1] $\mathbb{I}$ denotes the identity matrix with appropriate dimensions.

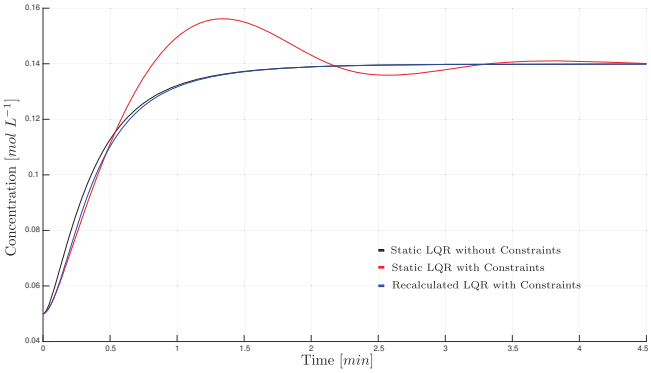

Fig. 10: Concentration time response.

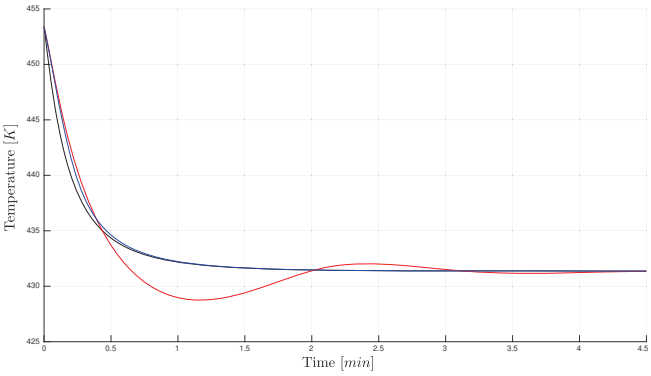

Fig. 11: Temperature time response.

Also, in red line, it presents the system response with the same state disturbance, when a static LQR with constraints on the manipulated variable is applied. Clearly the maximum value of the manipulated variable is not exceeded. Obviously this option, it has a lower performance than the previous case.

Finally, in blue line, it shows the system response to the state disturbance when a variable gain LQR with constraints on the control signal is applied. It is observed that with this regulator the system has a good performance and that the upper bound on manipulated variable is not exceeded.

Table III summarizes a comparison of the performance indexes of these three methods. It is possible to appreciate that regulator 1 has a similar performance to the regulator 3 while the regulator 2 presents higher Integral of Absolute Error (IAE), Time-weighted Integral of Absolute Error (ITAE) and Integral of Square Error (ISE) than the others ones.

TABLE III: Performance indexes of the implemented LQRs in a CSTR for the first test.

	Regulator	IAE	ITAE	ISE
1	Static LQR without Constraints	**0.039725**	$+1,497\%$	**0.0019287**
2	Static LQR with Constraints	$+7,368\%$	$+34,388\%$	$+8,026\%$
3	Recalculated LQR with Constraints	$+0,5387\%$	**0.016717**	$+2,810\%$

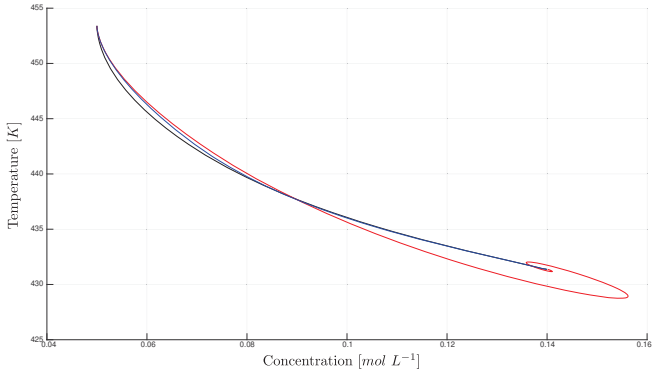

Fig. 12: State space.

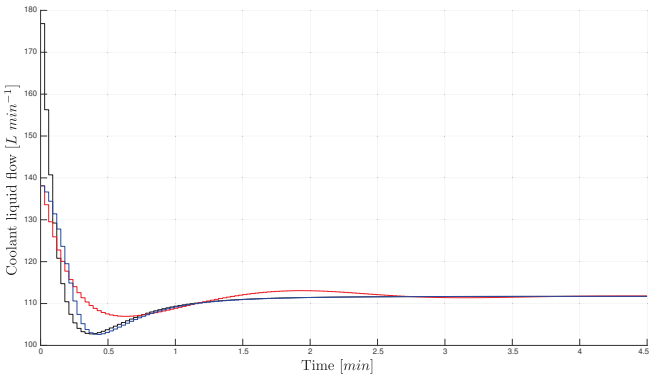

Fig. 13: Coolant flow rate.

The reason for this similar behavior in the system response, when the regulators 1 and 3 are applied, is due to the control signal constraint takes effect only at the initial instant, when the disturbance is maximum. Then, as the system evolves and approaches its equilibrium state, the required coolant flow is lower and this constraint no longer has effects. Therefore, when recalculating the gain at subsequent instants, both algorithms match and the gains are similar.

This can be seen in Figs. 14 and 15 where the gain of the three mentioned regulators is shown as a function of the iterations.

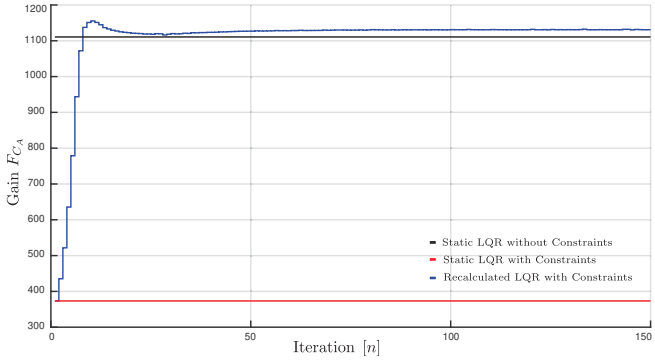

Fig. 14: Concentration control loop gain.

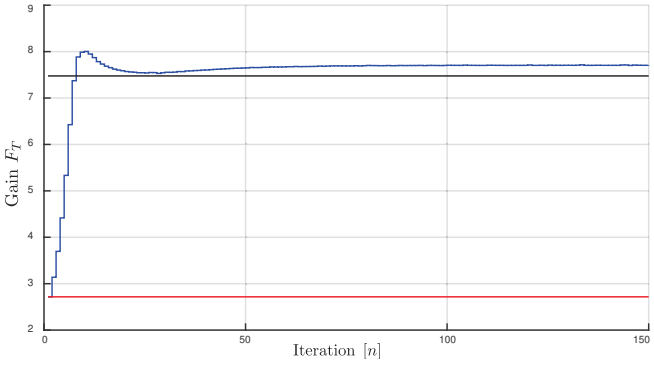

Fig. 15: Temperature control loop gain.

VI. Conclusion

In this work, a procedure to reduce the size of a large polytope without loss of robustness was presented as the main contribution. Moreover, the resulting reduced polytope was employed for the robust design of quadratic linear regulators, as demonstrated through numerical simulations, obtaining attractive results.

References

[1] E. J. Adam, *Instrumentación y Control de Procesos. Notas de Clase*, 3rd ed. Ediciones UNL, 2020.

[2] K. J. Aström and R. H. Murray, *Feedback Systems. An Introduction for Scientists and Engineers*. Princeton University Press, 2008.

[3] D. E. Seborg, T. F. Edgar, D. A. Mellichamp, and F. J. Doyle III, *Process Dynamics and Control*. John Wiley & Sons, 2011.

[4] S. Skogestad and I. Postlethwaite, *Multivariable Feedback Control - Analysis and Design*, 2nd ed. Wiley, 2005.

[5] H. A. Pipino, M. M. Morato, E. Bernardi, E. J. Adam, and J. E. Normey-Rico, "Nonlinear temperature regulation of solar collectors with a fast adaptive polytopic lpv mpc formulation," *Solar Energy*, vol. 209, pp. 214–225, 2020.

[6] S. Mate, H. Kodamana, S. Bhartiya, and P. S. V. Nataraj, "A stabilizing sub-optimal model predictive control for quasi-linear parameter varying systems," *IEEE Control Systems Letters*, 2019.

[7] H. A. Pipino, C. A. Cappelletti, and E. J. Adam, "Adaptive multi-model predictive control applied to continuous stirred tank reactor," *Computers & Chemical Engineering*, vol. 145, p. 107195, 2021.

[8] R. Tóth, *Modeling and identification of linear parameter-varying systems*. Springer, 2010, vol. 403.

[9] J. Mohammadpour and C. W. Scherer, *Control of linear parameter varying systems with applications*. Springer Science & Business Media, 2012.

[10] C. A. Cappelletti, E. Bernardi, H. Pipino, and E. J. Adam, "Optimum Multiobjective Regulator with Variable Gain Matrix Applied to an Industrial Process," *2018 Argentine Conference on Automatic Control, AADECA 2018*, 2018.

[11] J. D. Morningred, B. E. Paden, D. E. Seborg, and D. A. Mellichamp, "An Adaptive Nonlinear Predictive Controller," *Chemical Engineering Science*, vol. 47, no. 4, pp. 755–762, 1992.

[12] J. S. Shamma, "An overview of lpv systems," in *Control of linear parameter varying systems with applications*. Springer, 2012, pp. 3–26.

[13] K. Tanaka and H. O. Wang, *Fuzzy Control Systems Design and Analysis: A Linear Matrix Inequality Approach*. Wiley, 2001.

[14] Z. Wan and M. V. Kothare, "Efficient scheduled stabilizing model predictive control for constrained nonlinear systems," *International Journal of Robust and Nonlinear Control*, vol. 13, no. 3-4, pp. 331–346, 2003.

[15] M. V. Kothare, V. Balakrishnan, and M. Morari, "Robust Constrained Model Predictive Control Using Linear Matrix Inequalities," *Automatica*, vol. 32, pp. 1361–1379, 1996.

[16] J. Löfberg, "YALMIP : a toolbox for modeling and optimization in MATLAB," *2004 IEEE International Conference on Robotics and Automation (IEEE Cat. No.04CH37508)*, pp. 284–289, 2004.